THE ALTITUDE PROFILE OF IONOSPHERIC CURRENTS AND CONDUCTIVITIES DEDUCED FROM EISCAT OBSERVATIONS

Mariko Sato[1], Yohsuke Kamide[1], Asgeir Brekke[2] and Satonori Nozawa[1]

[1]*Solar-Terrestrial Environment Laboratory, Nagoya University, 3–13, Honohara, Toyokawa 442*
[2]*Auroral Observatory, University of Tromsø, N-9037 Tromsø, Norway*

Abstract: On the basis of updated EISCAT observations, the altitude profile of ionospheric currents and conductivities is examined. It is shown that the altitude distribution of the substorm westward electrojet changes quite dynamically, depending on the electrojet phases and also on local time. The altitude at which the current density and the Hall conductivity are maximized in morning hours is lower than that at midnight, indicating that energies of precipitating electrons are relatively high in the morning sector. The altitude distribution is also found to vary systematically in relation to the electrojet phases in the morning sector: the characteristic energies of precipitating electrons tend to increase during the electrojet recovery phase.

1. Introduction

Incoherent scatter radars are a powerful tool to study the electrodynamics of the ionosphere and to discuss the extent to which the ionosphere and the magnetosphere are electrically coupled. Radar observations provide us with the simultaneous determination of a number of ionospheric parameters, such as ionospheric electric fields and currents as well as the Hall and Pedersen conductivities (e.g., Banks and Doupnik, 1975; Röttger, 1991 for reviews).

With the Chatanika, Alaska, incoherent scatter radar, which was operated from 1971 to 1982, different types of experiments were performed, yielding, for example, the altitude structure of the *E*-region ionosphere from the observed electron density and the ion velocity (Banks *et al.*, 1974; Brekke *et al.*, 1974; Rino *et al.*, 1977; Brekke and Rino, 1978). On the basis of the Chatanika radar short-pulse experiment with an integration time of one min, Banks *et al.* (1974) presented altitude profiles of the observed electron density as well as time variations of the height of the maximum electron density. They were able to obtain some average notion about changes in the height of the *E*-layer in association with enhanced geomagnetic activities, however, there was an uncertainty surrounding the "true" height of the peak electron density (see Fig. 8 in Banks *et al.*, 1974).

The altitude distribution of ionospheric current vectors deduced from the observed electron density and the ion velocity was first obtained by Rino *et al.* (1977) by using single-pulse correlation techniques. A serious limitation with this technique was, however, the reduced sensitivity obtained due to the high resolution of 10 and 24 km in height achieved.

The European Incoherent Scatter Radar (EISCAT), which has been operated since 1981, is the only tristatic incoherent scatter radar facility in the world. Simultaneous observations of scattered signals at three receiving sites, located close to Tromsø in Norway, Kiruna in Sweden, and Sodankylä in Finland, allow the unambiguous determination of ion velocity vectors. BREKKE et al. (1990) showed the results of updated EISCAT CP(Common Program)-1 experiments. With a high time and space resolution, one can estimate directly the current densities at different heights in the E-region ionosphere, compared to the "single points" estimate as obtained by BREKKE et al. (1974).

More recently, on the basis of measurements of CP-1 version I, the distribution of ionospheric current vectors at six different altitudes in the E-region has been presented by KAMIDE and BREKKE (1993). It has been shown that current vectors at different altitudes are very different, particularly during polar substorms. The primary purpose of this report is to attempt to show, by using the CP-1 data, that the altitude distribution of the ionospheric current and the conductivity in the eastward and westward electrojets changes systematically in relation to the electrojet phases.

2. Data Presentations

A detailed description of the EISCAT radar CP-1 mode is given in RISHBETH and WILLIAMS (1985). The CP-1 mode observations use a fixed transmitting direction along the local magnetic field (the elevation angle of 76.5° to south) to measure electron densities, electron and ion temperatures, and velocities as functions of altitude. A full, three-dimensional ion velocity vector is measured with the CP-1 experiments at six different altitudes, at 90, 96, 101, 109, 117, and 124 km in the E-region and at 278 km in the F-region. It takes approximately 10 min for the radar system to obtain a full set of ion velocity vectors at the seven heights with an integration time of one min. These parameters can then be used to determine current densities, Hall and Pedersen conductivities, and electric fields in the ionosphere.

The ionospheric current density $j(z)$ at height z is given by

$$j(z) = N_e(z) \cdot e \cdot (\mathbf{v}_i(z) - \mathbf{v}_e(z)), \tag{1}$$

where $N_e(z)$ is the electron density at height z, e is the charge of electrons, $\mathbf{v}_e(z)$ and $\mathbf{v}_i(z)$ are the electron and ion velocities at height z, respectively. It is assumed that the electron velocity is constant above about 90 km, being equal to the $\boldsymbol{E} \times \boldsymbol{B}$ drift, because the electron-neutral collision can be neglected. We also assume that the ion velocity in the F-region (278 km) is equal to the electron velocity, the $\boldsymbol{E} \times \boldsymbol{B}$ drift. The electric field hence can be deduced from the ion velocity measured at 278 km (see BREKKE et al., 1990).

Following BREKKE et al. (1974), the Hall and Pedersen conductivities are expressed as:

$$\sigma_{\mathrm{H}} = \frac{N_e e}{B} \left(\frac{\omega_e^2}{\omega_e^2 + \nu_e^2} - \frac{\omega_i^2}{\omega_i^2 + \nu_i^2} \right), \tag{2}$$

$$\sigma_P = \frac{N_e e}{B} \left(\frac{\omega_i v_i}{\omega_i^2 + v_i^2} - \frac{\omega_e v_e}{\omega_e^2 + v_e^2} \right), \tag{3}$$

where ω_i and ω_e are the ion and electron gyrofrequencies, respectively; and v_i and v_e are the altitude-dependent ion-neutral and electron-neutral collision frequencies, respectively. Here we use the model by Schunk and Walker (1973) for the ion-neutral collision frequency and that by Schunk and Nagy (1978) for the electron-neutral collision frequency.

3. Results

Figure 1a shows the current density vectors perpendicular to the magnetic field. These are calculated from (1) and are presented as vector arrows at six different heights in the E-region ionosphere. The height-integrated current vectors are also shown at the bottom of the current diagram. This particular experiment covers a 24 h period starting at 1000 UT on April 9, 1990. The magnetic local time (MLT) at the EISCAT site, Tromsø, relates to UT as MLT≈UT+2 h.
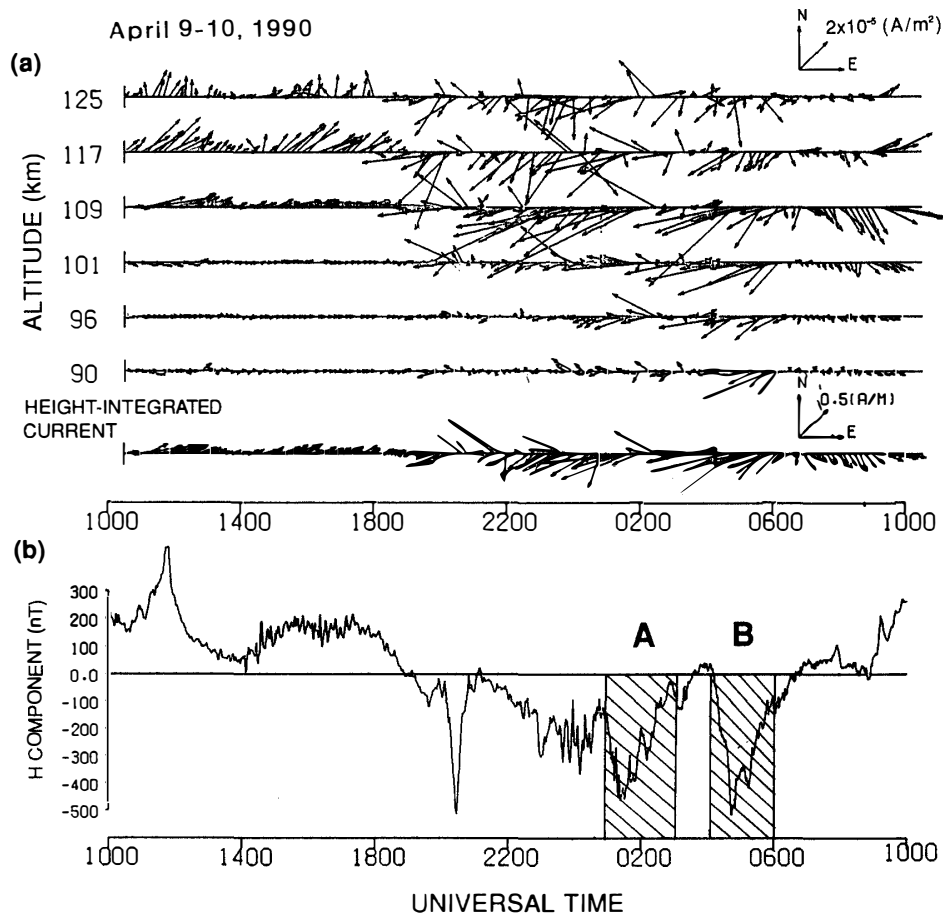

Fig. 1. (a) Vectors of the current density at six different heights on April 9–10, 1990, and vectors of height-integrated ionospheric currents at the bottom of the diagram. (b) Magnetic variations in the H component at Tromsø.

The geomagnetic H component, which is measured from the average value during one of the quietest days, April 8, is shown in Fig. 1b. The day, presented in Fig. 1, appears to be rather disturbed with occurrence of several substorms. The eastward electrojet, which causes positive geomagnetic disturbances of about 200 nT in the H component, is observed in the evening sector, whereas several strong enhancements in the westward electrojet are present in the midnight and morning sectors. While the strong enhancements in the H component are detected, highly variable Z perturbations are observed. In fact, ΔZ is fluctuating wildly between positive and close to zero values while ΔH is negative. This indicates that the center of the westward electrojet is located south of or near Tromsø.

It is clear that the altitudinal characteristics of the eastward and westward electrojets are quite different. The height range for the westward electrojet is much larger than that for the eastward electrojet. The altitude dependence is highly variable in the westward electrojet, while the eastward electrojet is quite stable over the altitude range that was covered by the radar. As is evident in Fig. 1a, the current center of the eastward electrojet is located at higher altitudes than that of the westward electrojet. This result is consistent with an earlier observation of KAMIDE and BREKKE (1977), who used data from the Chatanika radar.

It is important to point out that the altitudinal characteristics of the westward electrojet vary considerably at different local times and at the different electrojet phases. To examine the local time dependence of the altitude profiles, we have taken averages of the current density and the Hall conductivity over the intervals in the midnight sector, period A (0100–0300 UT), and in the morning sector, period B
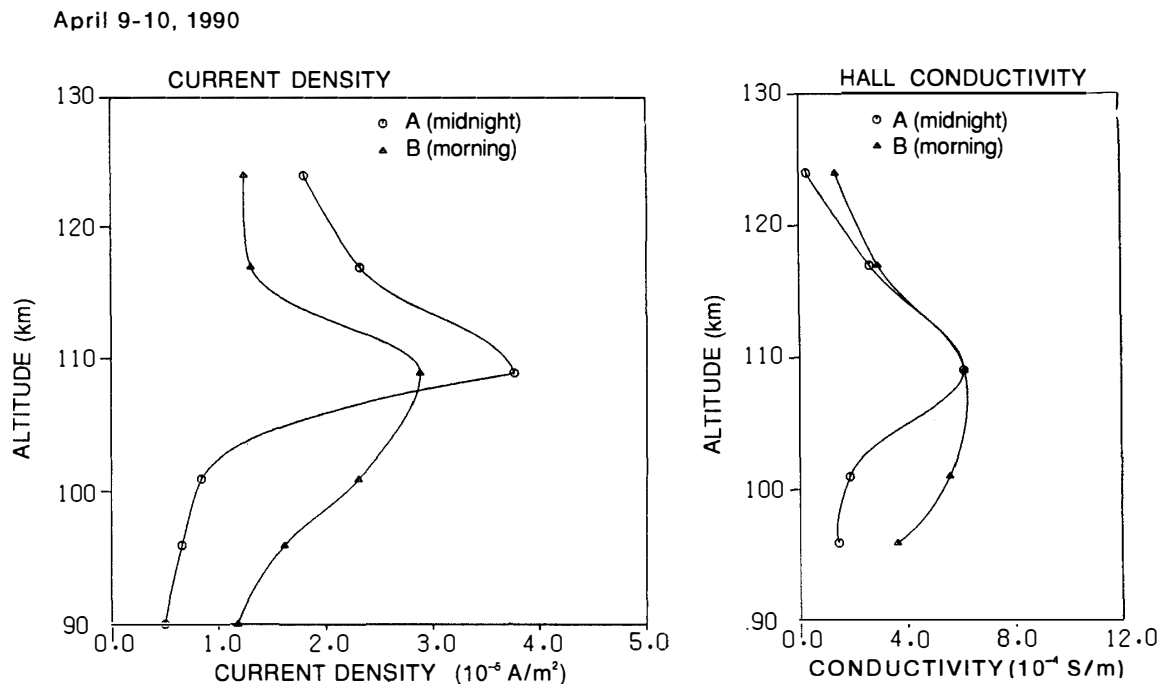
April 9-10, 1990

Fig. 2.   Altitude profiles of the current density (left) and the Hall conductivity (right) in the midnight and morning sectors.

(0400–0600 UT). These two intervals are marked with hatches in Fig. 1b. The negative H component perturbations observed on the ground reached about −400 nT during both of these intervals.

Figure 2 (left) shows the altitude profiles of the averaged current density in the midnight and morning sectors. The right-hand side of Fig. 2 is for the Hall conductivity. Open circles and triangles designate the values in the midnight sector and in the morning sector, respectively. It is clear from Fig. 2 that the vertical distribution in the morning sector differs from that in the midnight sector. At lower altitudes, about 100 km, the current density as well as the Hall conductivity in the morning sector is about three times as intense as that in the midnight sector, while they decrease at higher altitudes. This indicates that energies of precipitating electrons are relatively high in the morning sector. Earlier studies support this result (e.g., Brekke et al., 1989). In their paper Brekke et al. (1989) presented the Hall-to-Pedersen conductance ratio, which is corrected to remove the effects of the background ionization caused by the solar UV, showing that the ratio is much higher in the morning sector than that in the midnight sector.

It is also of great interest to see time variations of the altitude profiles of the current density and the corresponding Hall conductivity during strong electrojet activity. Figure 3a shows H component magnetic perturbations in morning hours at Tromsø. For the present study, variations in the altitude profiles of the current density are examined for two different electrojet phases. Here we use the term "electrojet expansion phase" to mean periods, such as Period C indicated in Fig. 3a, where the westward ionospheric current suddenly increases. The simultaneous H component decreases rapidly during the electrojet expansion phase. Note that this dose not necessarily mean that the substorm was in the expansion phase on a global scale. In a similar fashion, we use the term "electrojet recovery phase" to refer to intervals, such as Period D, during which the H component returns to the pre-disturbed level.

Figure 3b shows the altitude profiles of the current density and the Hall conductivity during the electrojet expansion and recovery phases. Each profile indicates average values taken over the intervals which are marked with hatches in Fig. 3a. The average values during the expansion phase and during the recovery phase are indicated by open circles and triangles, respectively. It is seen that the altitude at which the current density as well as the Hall conductivity is maximized shifts toward lower altitudes (about 100 km) from the expansion to recovery phases. This indicates that energies of precipitating particles during the electrojet recovery phase are higher than those during the electrojet expansion phase. This nature is found to be common in our data set, especially in the morning-side electrojet.

To discuss the variation of the altitude profile of the ionospheric conductance, it is worthwhile to point out the importance of the characteristic energy of auroral electrons. The ionization profile reflects the characteristic energies of the precipitating particles. From the measured electron density profile and the computed ionization profile, one can estimate the differential energy spectrum of the incident auroral electrons (Vondrak and Baron, 1976; Brekke et al., 1989; Hargreaves and Devlin, 1990). The enhanced ionization at 110 km and 101 km is caused by the energetic
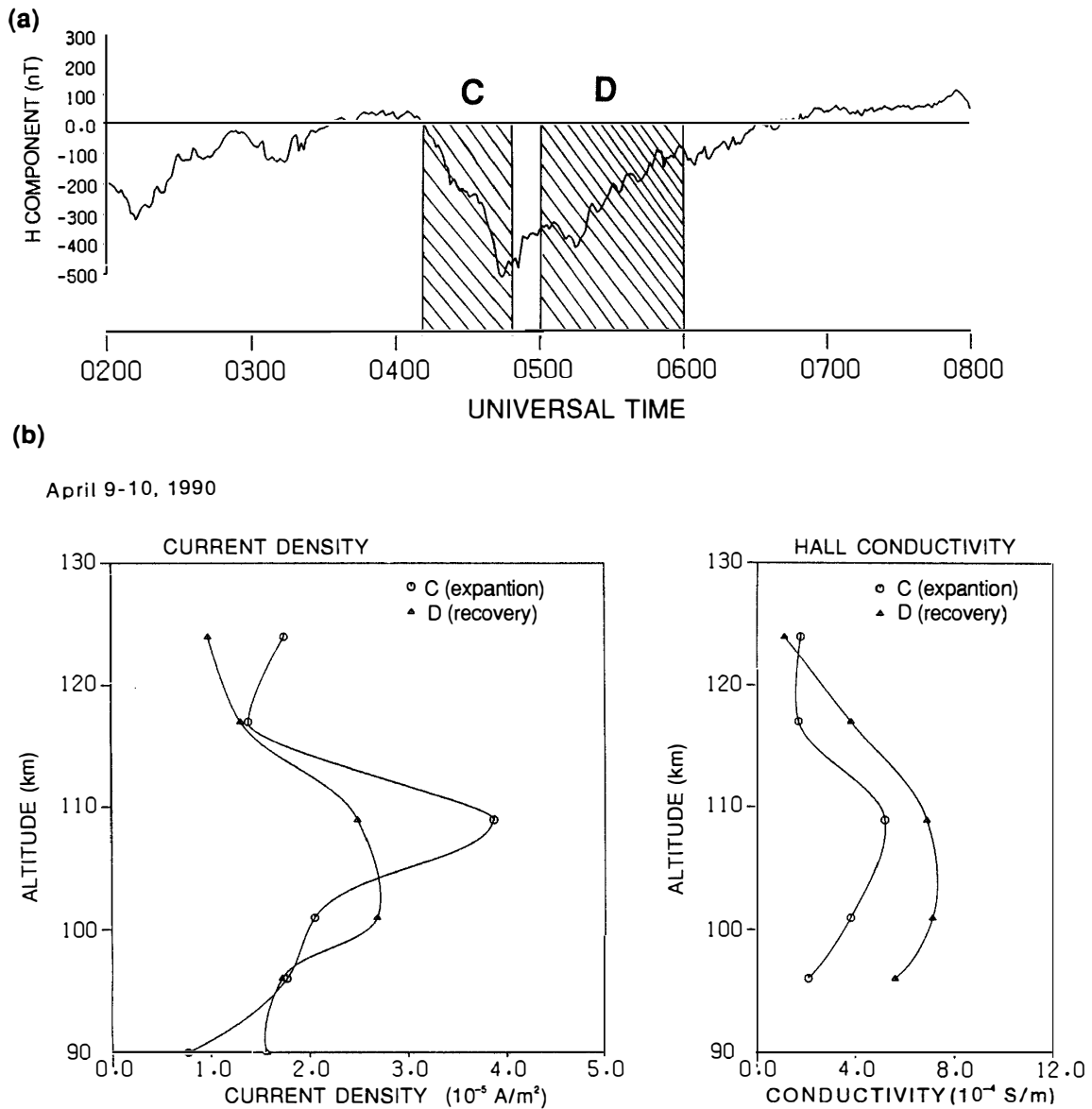
(a)

(b)

April 9-10, 1990

Fig. 3.   (a) Magnetic variations in the H component at Tromsø in the morning sector (0200–0800 UT). (b) Altitude profiles of the current density (left) and the Hall conductivity (right) during the electrojet expansion and recovery phases.

electrons with energies of about 7 keV and 10 keV, respectively (e.g., VONDRAK and BARON, 1976). In our case, the characteristic energy of precipitating electron is about 10 keV during the electrojet recovery phase, whereas it is about 7 keV during the expantion phase.

Concerning the characteristic energy of precipitating particles, we must excise caution on the spatial distribution of precipitating particles. ROSTOKER et al. (1985) related the spectral characteristics of the precipitation of energetic electrons across the latitudinal extent of the auroral oval to the location of the ionospheric electrojets in the morning sector. Data of energetic electron, obtained with the Isis 2 satellite,

were organized into four distinct regions as a function of latitude: for a detailed description of the spectral characteristics of the electrons at these regions, see Ros-TOKER *et al.* (1985). The region which contains fluxes of relatively hot electrons is Region C, which is found to be colocated with the equatorward portion of the westward electrojet. Region B appears to map into the poleward portion of the electrojet. The differential energy distribution of electrons in Region B represents little evidence of near-monoenergetic peaks. Average energies of electrons in Region C are noticeably higher than those in Region B.

It is important to recognize that these latitudinal regimes move relative to the EISCAT site according to different states of geomagnetic activity, although the boundary between Region B and Region C tends to be located, in general, near the EISCAT site under disturbed conditions. Since the CP-1 observations use a fixed transmitting direction, it is difficult to determine in which latitudinal region the radar is located. In any case, although it has been found to be common for the altitude profiles to vary significantly, depending on the electrojet phases, this finding may also be explained by taking into account variations of the latitudinal distribution of the auroral electrojet, which changes with the phases. We plan to inquire into this subject in the near future.

4. Summary

On the basis of updated EISCAT CP-1 observations, we have studied the altitude distribution of the current density and the conductivities in the E-region ionosphere. It has been found that the altitude profiles of the current density and the Hall conductivity change considerably, depending on local time. The altitude at which the current density and the Hall conductivity are most intense in the morning sector is lower than that in the midnight sector, indicating that energies of precipitating particles in the morning sector are, on average, higher than those in the midnight sector. In view of some of the earlier observations, this may not be unexpected.

We have also found that variations of the altitude distribution appear to depend on the electrojet phases. The peak altitudes of the current density and the Hall conductivity tend to shift toward lower altitudes over periods from the electrojet expansion to recovery phases. This implies that particles with relatively high energies precipitate during the electrojet recovery phase. It must be cautioned, however, that this finding can be accounted for also by considering either that the latitudinal distribution of precipitating particles varies during substorms, or that the auroral electrojet moves latitudinally with respect to the radar location, or both. It is quite conceivable that all these can occur throughout individual substorms. It is necessary in the near future to examine the relative location of the electrojets with respect to the EISCAT site as well as its time variations, on the basis of magnetic data from the Scandinavia meridian chain of observatories.

Acknowledgments

these valuable sets of Common Program data.   One of the authors (M.S.) would like to thank the Auroral Observatory, University of Tromsø for its hospitality as well as financial support for her staying at Tromsø for one month in winter 1993.   This work was supported in part by the National Institute of Polar Research.

References

BANKS, P. M., RINO, C. L. and WICKWAR, V. B. (1974): Incoherent scatter radar observations of westward electric fields and plasma densities in the auroral ionosphere.   J. Geophys. Res., **79**, 187–198.

BANKS, P. M. and DOUPNIK, J. R. (1975): A review of auroral zone electrodynamics deduced from incoherent scatter radar observations,.   J. Atmos. Terr. Phys., **37**, 951–972.

BREKKE, A., DOUPNIK, J. R. and BANKS, P. M. (1974): Incoherent scatter measurements of E region conductivities and currents in the auroral zone.   J. Geophys. Res., **79**, 3773–3790.

BREKKE, A. and RINO, C. L. (1978): High-resolution altitude profiles of the auroral zone energy dissipation due to ionospheric currents.   J. Geophys. Res., **78**, 2517–2524.

BREKKE, A., HALL, C. and HANSEN, T. L. (1989): Auroral ionospheric conductances during disturbed conditions.   Ann. Geophysicae, **7**, 269–280.

BREKKE, A., HALL, C. and PETTERSEN, Ø. (1990): EISCAT UHF studies of ionospheric currents on June 16–17, 1987.   Ann. Geophysicae, **8**, 213–222.

HARGREAVES, J.K. and DEVLIN, T. (1990): Morning sector electron precipitation events observed by incoherent scatter radar.   J. Atmos. Terr. Phys., **37**, 951–972.

KAMIDE, Y. and BREKKE, A. (1977): Altitude of the eastward and westward auroral electrojets.   J. Geophys. Res., **82**, 2851–2853.

KAMIDE, Y. and BREKKE, A. (1993): Altitude variations of ionospheric currents at auroral altitudes.   Geophys. Res. Lett., **20**, 309–312.

RINO, C.L., BREKKE, A. and BARON, M. J. (1977): High-resolution auroral zone E region neutral wind and current measurements by incoherent scatter radar.   J. Geophys. Res., **82**, 2295–2304.

RISHBETH, H. and WILLIAMS, P. J. S. (1985): The EISCAT ionospheric radar : The system and its early results.   Q. J. R. Astron. Soc., **26**, 478–512.

ROSTOKER, G., KAMIDE, Y. and WINNINGHAM, J. D. (1985): Energetic particle precipitation into the high-latitude ionosphere and the auroral electrojets.   3. Characteristics of electron precipitation into the morning sector auroral oval.   J. Geophys. Res., **90**, 7495–7504.

RÖTTGER, J. (1991): Incoherent scatter observations of the auroral ionosphere with the EISCAT radar facility.   Auroral Physics, ed. by C.-I. MENG *et al.*   Cambridge, Cambridge Univ. Press, 419–437.

SCHUNK, R. W. and WALKER, J. C. G. (1973): Theoretical ion densities in the lower ionosphere.   Planet. Space Sci., **21**, 1875–1896.

SCHUNK, R. W. and NAGY, A. F. (1978): Electron temperatures in the F-region of the ionosphere: Theory and observations.   Rev. Geophys. Space Phys., **16**, 355–399.

VONDRAK, R. R. and BARON, M. J. (1976): Radar measurements of the latitudal variation of auroral ionization.   Radio Sci., **11**, 939–946.